IEEE Access
Multidisciplinary | Rapid Review | Open Access Journal

Received July 12, 2018, accepted August 1, 2018, date of publication August 7, 2018, date of current version August 28, 2018.

Digital Object Identifier 10.1109/ACCESS.2018.2864169

Collision Avoidance in Fixed-Wing UAV Formation Flight Based on a Consensus Control Algorithm

JIALONG ZHANG[1], JIANGUO YAN[1], PU ZHANG[1], AND XIANGJIE KONG[2], (Senior Member, IEEE)

[1]School of Automation, Northwestern Polytechnical University, Xi'an 710129, China
[2]Key Laboratory for Ubiquitous Network and Service Software of Liaoning Province, School of Software, Dalian University of Technology, Dalian 116620, China

Corresponding author: Jialong Zhang (zjl0117@mail.nwpu.edu.cn)

This work was supported by the National Natural Science Foundation of China under Grant 60974146 and Grant 61473229.

ABSTRACT This paper addresses a collision avoidance problem for multiple unmanned aerial vehicles (UAVs) in the process of high-speed flight, thereby enabling UAV cooperative formation flight and effective mission completion. The main contribution is to propose a collision avoidance control algorithm for a multi-UAV system based on a bi-directional network connection structure. To effectively avoid collisions between UAVs and between UAVs and obstacles, the proposed consensus-based algorithm and a ''leader-follower'' control strategy are simultaneously applied for UAV formation control to ensure the convergence of the formation. Each of the UAVs has the same forward velocity and heading angle in the horizontal plane, and they maintain a constant relative distance in the vertical direction. This paper proposes a consensus-based collision avoidance algorithm for multiple UAVs based on an improved artificial potential field method. Simulation tests involving multiple UAVs were performed to validate the proposed control algorithm and to provide a reference for engineering applications.

INDEX TERMS Bidirectional network connection, consensus -based control algorithm, collision avoidance, algorithm validation, engineering application.

I. INTRODUCTION

The obstacle avoidance problem for a multi-UAV formation system has been extensively studied in recent years, and many control algorithms have been developed and proposed to address this problem. Obstacle avoidance control algorithms can be roughly grouped into two categories: rule-based approaches and optimization-based approaches. One example of a rule-based approach is the artificial potential field based approach [1], [2]. Meanwhile, the classic example of an optimization-based approach is model predictive control (MPC) [3]. During formation control, the main control algorithm is applied in combination with consensus-based control theory to achieve good controller design. The consensus-based algorithm for the UAV cooperative formation control is a kind of distributed control method, which has the advantage of flexibility in terms of network structure [4]–[7] and can achieve multi-channel compound control obstacle avoidance. The so-called consensus algorithm means that each of the UAVs has a constant relative position and the same attitude under a certain control protocol, which can achieve the purpose of the cooperative collision avoidance. The key question that arises with regard to the obstacle avoidance control of a multi-agent system is how to apply a consensus-based algorithm to effectively cope with the problem [8]–[10], as doing so would greatly reduce the problem complexity. The dynamics of a multi-UAV system can be modeled as a fourth-order system on the horizontal plane and a separate second-order system in the vertical direction [11].

In practical engineering, collision avoidance control algorithms have been applied to real-world UAV formations by many researchers. Jennifer *et al.* [12] considered a collision avoidance problem between two aircrafts in a three-dimensional environment using a combination of a geometric approach and a collision-cone approach, and they proposed a guidance law based on the collision-cone approach. Choi *et al.* [13] proposed a vision-based collision avoidance system for a single UAV using a single sensor. Portilla *et al.* [14] performed a feasibility study for a collision avoidance algorithm compatible with the Traffic Alert and Collision Avoidance System used for manned aircraft.

Fasano *et al.* [15] presented a fully autonomous multi-sensor anti-collision system for UAVs with collision geometry with the purpose of detecting and avoiding obstacles and generating feasible trajectories in real time.

To effectively solve the obstacle avoidance problem, this study proposes a consensus-based collision avoidance algorithm. The main contributions of this study, relative to other works, are as follows:

1) We use the same simple model of a single UAV or a UAV formation in this paper, and the consensus-based algorithm we proposed also has the advantageous feature of effective collision avoidance in three-dimensional space. In addition, the consensus-based algorithm guarantees that the UAV formation will converge to the desired path while maintaining a safe distance between any nearby obstacle and the central UAV in the formation; that is, the relative distance error between them converges to a small, stable value.

2) Many researchers have proposed consensus-based control algorithms that guarantees convergence to the desired formation flight path. However, the control algorithm presented in [16] was designed for formation flight only in a horizontal plane, not in three-dimensional space. In this study, the control algorithm we propose can also effectively avoid obstacles in the vertical direction, thus making it more widely applicable and flexible than the algorithms proposed by other scholars. In this paper, we propose to combine a consensus algorithm based on an improved artificial potential field method with a ''leader-follower'' control strategy for application to a system consisting of three UAVs in formation.

3) Simulation results from a semi-physical simulation platform demonstrate good in-flight stability. The next major task will be to apply our proposed approach to a real UAV formation to test its ability to effectively avoid obstacles in three-dimensional space; however, this paper presents only a theoretical study.

The rest of this paper is organized as: In Sec. II, we present the modeling of a single UAV and a three-UAV formation and define the control objectives. In Sec. III, we propose the control methods for the models built in Sec. II. In Sec. IV, we propose the control algorithms for avoiding collisions between the UAV formation and obstacles and between the UAVs. In Sec. V, we further study how to avoid obstacles during formation flight based on the artificial potential field method and two kinds of collision avoidance schemes. Sec. VI presents experiments to validate that the proposed control algorithm can effectively achieve collision avoidance. Finally, concluding remarks are provided in Sec. VII.

II. PROBLEM STATEMENT

This paper considers a regular triangular UAV formation consisting of three fixed-wing UAVs, including a leader and two followers. They are placed at the three vertices of a regular triangle and are treated as the control object. Each UAV is equipped with a position sensor, and they can share specific position with each other via bidirectional information flows, constituting a bidirectional network structure. During the multi-UAV cooperative formation flight, when the UAV formation comes close to a static or moving obstacle, a consensus-based collision avoidance algorithm is run that is embedded in the UAV controller, the measurements of the UAV position sensors are used to cause the UAVs to take evasive action. The collision avoidance algorithm ensures that the relative distance between the obstacle and the UAV that is nearest to the obstacle is greater than the safe distance between them to successfully achieve collision avoidance with the optimal path. In Sec. III, we present the mathematical modeling of a linearized UAV in the vertical direction and a multi-UAV system, and we define the control objectives.

III. UAV FORMATION CONTROL

The regular triangular UAV formation considered as the control object consists of two followers and a leader in this paper. An improved artificial potential field algorithm is proposed for UAV formation control to achieve collision avoidance in three-dimensional space.

A. MODELING A SINGLE UAV

Suppose that there are N (N>1) UAVs with the same dynamic characteristics, including N-1 followers and a leader, which together compose a multi-UAV formation system. Each of the UAVs is equipped with a complete set of communications equipment and controllers, and each follower receives control commands from the leader and executes the corresponding maneuvers. To build a simple model of such a UAV, let us make four assumptions, as follows. First, the dynamic response time between the leader sending a command and the follower receiving the command can be ignored. Second, the UAV flies slowly enough that external aerodynamic forces acting on the UAV, such as aerodynamic drag and blade-vortex interaction, can be ignored. Third, to maintain the geometric configuration of the UAV formation, each UAV is treated as a rigid body. Fourth, when hovering at a constant altitude, the UAV is in a state corresponding to an equilibrium point of a nonlinear system, which can be decoupled into linear systems in the longitudinal, lateral and vertical directions. This paper focuses on the linear systems in the lateral and vertical directions, so a mathematical model of a single UAV can be built as follows [17]–[20]. First, the continuous horizontal mathematical model of a single UAV, including the lateral, roll and pitch moments, is given by

$$\left(\frac{d}{dt} - Y_v\right)\Delta v - Y_p\Delta p + (u_o - Y_r)\Delta r - g\cos(\theta_o)\Delta\phi = Y_{\delta r}\Delta\delta r \tag{1}$$

$$-L_v\Delta v + \left(\frac{d}{dt} - L_p\right)\Delta p - \left(\frac{L_{xz}}{I_x}\frac{d}{dt} + L_r\right)\Delta r = L_{\delta\alpha}\Delta\delta\alpha + L_{\delta r}\Delta\delta \tag{2}$$

$$-N_v\Delta v - \left(\frac{L_{xz}}{I_Z}\frac{d}{dt} - N_p\right)\Delta p + (\frac{d}{dt} - N_r)\Delta r = N_{\delta\alpha}\Delta\delta\alpha + N_{\delta r}\Delta\delta r \tag{3}$$

$$\dot{X} = AX + Bu \tag{4}$$

where

$$A = \begin{bmatrix} Y_v & Y_p & Y_r - \mu_0 & g\cos\theta_0 \\ L_v^T \frac{I_{xz}}{I_x} N_v^T & L_p^T \frac{I_{xz}}{I_x} N_v^p & L_r^T \frac{I_{xz}}{I_x} N_r^T & 0 \\ N_v^T \frac{I_{xz}}{I_x} L_v^T & N_p^T \frac{I_{xz}}{I_x} L_p^T & N_r^T \frac{I_{xz}}{I_x} L_r^T & \\ 0 & 1 & 0 & 0 \end{bmatrix}$$

$$B = \begin{bmatrix} 0 & Y_{\delta r} \\ N_{\delta\alpha}^T & +\frac{I_{xz}}{I_x} L_{\delta\alpha}^T \quad L_{\delta r}^T & +\frac{I_{xz}}{I_x} L_{\delta r}^T \\ N_{\delta\alpha}^T & +\frac{I_{xz}}{I_Z} L_{\delta\alpha}^T \quad N_{\delta r}^T & +\frac{I_{xz}}{I_x} L_{\delta r}^T \\ 0 & 0 \end{bmatrix},$$

$$X = \begin{bmatrix} v \\ p \\ r \\ \phi \end{bmatrix}, \; u = \begin{bmatrix} \delta_\alpha \\ \delta_r \end{bmatrix}$$

Here, v is the airspeed (m/s), p is the roll rate (deg/s), q is the pitch rate (deg/s), r is the yaw rate (deg/s), θ is the pitch angle (deg), α is the attack angle, L is the lateral axis, δ_α is the attack angle of the command input signal, δ_γ is the yaw rate of the command input signal, Y is the y axis, and g is the constant of gravitational acceleration (m/s^2).

Under the assumption that the inertial product satisfies, Eqs. (1) to (3) simplify to

$$\begin{bmatrix} \dot{v} \\ \dot{p} \\ \dot{r} \\ \phi \end{bmatrix} = xz \begin{bmatrix} Y_v & Y_p & u_o - Y_r & g\cos\theta_0 \\ L_v & L_p & L_r & 0 \\ N_v & N_p & N_r & 0 \\ 0 & 1 & 0 & 0 \end{bmatrix} \begin{bmatrix} v \\ p \\ r \\ \phi \end{bmatrix} + \begin{bmatrix} 0 & Y_{\delta r} \\ L_{\delta\alpha} & L_{\delta r} \\ N_{\delta\alpha} & N_{\delta r} \\ 0 & 0 \end{bmatrix} \begin{bmatrix} \delta_\alpha \\ \delta_r \end{bmatrix} \tag{5}$$

In the vertical direction, the linear model of the UAV is as shown in Eq. (6) [21]:

$$\frac{d}{dt} \begin{bmatrix} h_i^{(0)} \\ h_i^{(1)} \end{bmatrix} = \begin{bmatrix} h_i^{(1)} \\ \tilde{T}_{total_i} \end{bmatrix}, \quad i \in \{1, 2, \cdots, N\} \tag{6}$$

where $h^{(0)} = h$, $h^{(1)} = -w$, and $\tilde{T}_{total_i} = T_{total}/m$. Here, h is the altitude (m), and w is the rate of descent (m/s) in the vertical direction, which is the projection of the flight speed onto the z axis, namely, the component of the speed in the direction of the z axis. Thus, w is also the speed along the z axis. T_{total} is the total commanded thrust, and m is the mass of each UAV (kg). The modeling a multi-UAV system is shown in [22].

B. CONTROL OBJECTIVES

In this paper, we desire that there should be no collisions between the two followers, between the leader and the followers, or between the UAVs and any moving or stationary obstacle during the execution of a combat mission. In addition, the formation system should converge to the expected trajectory while maintaining its triangular formation, and the expected time-varying trajectory is determined by the configuration of the formation; in other words, the path is defined by the leader. Moreover, how to select a leader or follower in formation is also very critical [23]–[25]. Three UAVs compose the formation system; the leader is in the front, and the two followers track the leader through commands sent by the leader such that a triangular formation is maintained. To better control the three UAVs during triangular formation flight, we make the following two assumptions:

Assumption 1: In the network topology, every follower can receive commands from the leader, and the communication between the two followers is also normal. In addition, the network connecting the UAVs must provide bidirectional connections.

Assumption 2: The movement of the leader is not affected by the two followers. Moreover, the communication between the leader of one formation and the leader of another formation is bidirectional.

IV. COLLISION AVOIDANCE CONTROL

During the multi-UAV formation flight, to prevent collisions between the UAVs and between the UAVs and obstacles, an obstacle avoidance control method is particularly important. In this paper, a leader-follower strategy and an improved artificial potential field method are simultaneously used to avoid collisions between UAVs and between the leader or a follower and a nearby obstacle.

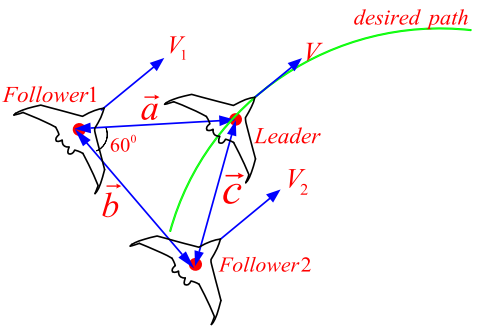

FIGURE 1. The "leader-follower" control model.

A. THE "LEADER-FOLLOWER" CONTROL STRATEGY

In this paper, a "leader-follower" model is adopted because of its flexibility and controllability. The control model is shown in Fig. 1. The leader receives commands from the ground command, whereas the two followers are each expected to maintain a desired distance and direction relative to the leader. To mitigate data transmission overload, we adopt a bidirectional network topology. In the formation, each UAV is defined, and their communication with each other is smooth, thereby effectively preventing excessive communications and the possibility of data transmission congestion among multiple UAVs.

To better control the UAV formation in accordance with the desired flight trajectory, we propose the simultaneous execution of an outer loop and an inner loop. The primary purpose of the outer loop is to cope with the relationship between the posture, forward velocity, and position of each UAV and the desired path. Meanwhile, the inner loop receives commands from the outer loop and then generates the aileron and rudder commands to ensure that the UAV can fly well at the desired altitude. Based on the above discussion, the detailed control diagram is as shown in Fig. 2. In this figure, the state vector x^T consists of the accelerations a_x, a_y, and a_z and the velocities p, q, and r along the three axes of the body frame of the UAV; the attitudes ψ, θ, and ϕ and the ground velocities u, v, and w on the three axes as well as the x, y, and h positions of the UAV are also included.

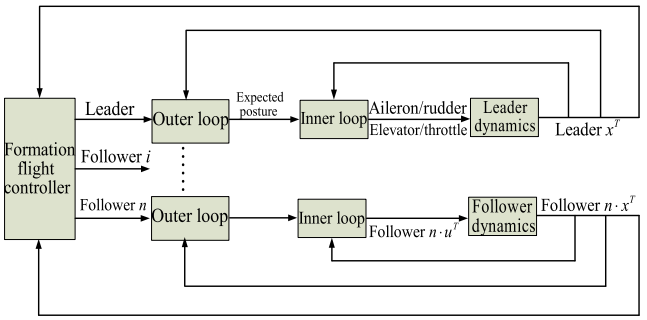

FIGURE 2. The "leader-follower" control diagram.

B. THE OBSTACLE AVOIDANCE CONTROL METHOD BASED ON ARTIFICIAL POTENTIAL FIELDS

In the triangular UAV formation considered here, the relative positions of the two followers and the leader have a certain symmetry. Hence, either the follower or the leader can be chosen as the control object, and the corresponding formation flight collision avoidance diagram is shown in Fig. 3.

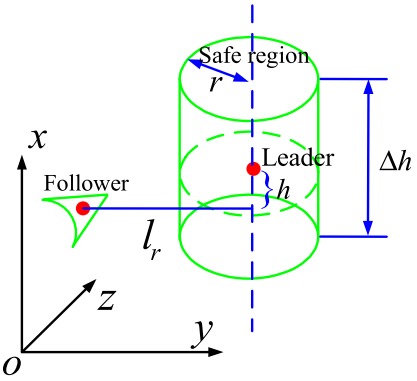

FIGURE 3. The formation flight collision avoidance diagram.

To achieve collision avoidance between the UAVs, we define the safe region for any UAV with the center of the leader as the center and r and Δh as the radius and height, respectively, of the cylindrical safe range. During the UAV formation flight, each UAV can fly within its respective safe region, and if there is an overlap between the UAVs' safe regions, they should take evasive action until this overlap is eliminated. Here, we define h and l_r as the relative altitude between a follower and the leader in the vertical direction and their relative separation in the horizontal plane, respectively. The relationship between the positions of the leader and the follower can be expressed as follows:

$$r_r = |r_l - r_f|, \quad h_a = \sqrt{(h_l - h_f)^2} \tag{7}$$

$$h_r = |h_l - h_f|, \quad r_a = \sqrt{(x_l - x_f)^2 + (y_l - y_f)^2} \tag{8}$$

Here, the symbol subscripts r, l, f and a denote the relative distance, the leader and the follower and the distance in the inertial coordinate system, respectively. In this paper, we define an improved artificial potential field between the leader and the follower as follows:

$$U_r = \begin{cases} \frac{k_h}{2}\left(\frac{1}{|h_r|+1} - \frac{1}{\Delta h+1}\right)^2, & |h_r| \le \Delta h \text{ or } |l_r| \le 2r \\ 0, & else \end{cases} \tag{9}$$

where $K_h \in R$ is a positive control parameter. The artificial potential field decreases as the vertical altitude gap between the UAVs decreases, and vice versa. In addition, when there is no overlap between the safe regions of the UAVs, the artificial potential between them is zero.

From the network topology of UAV formation system [22], we can obtain the average artificial potential field between the leader and the follower as follows:

$$U_i = \frac{1}{N-1}\sum_{j=1, j\neq i}^{N} U_{ij}, \quad i \in \{1, 2, \cdots, N+1\} \tag{10}$$

From Eq. (10), we can obtain the total artificial potential field of every UAV as follows:

$$U_c = \sum_{i=1}^{N} U_i \tag{11}$$

For a three-UAV formation, the total artificial potential field produced by the UAVs is given by

$$U_t = U_1 + U_2 + U_3 \tag{12}$$

where $U_1 = \frac{1}{2}(U_{12} + U_{13})$,$U_2 = \frac{1}{2}(U_{21} + U_{23})$ and $U_3 = \frac{1}{2}(U_{31} + U_{32})$.

To avoid collisions between the leader and the followers, an artificial force is proposed as follows:

$$f_{ca_i} = -\nabla h U_c, \quad i \in \{1, 2, \cdots, N\} \tag{13}$$

Note that there is no local minimum because the potential field consists only of repulsive potential fields. Its vector form is given by

$$f_{ca} = -\nabla U_c = -\left[\frac{\partial U_c}{\partial U_1}, \frac{\partial U_c}{\partial U_2}, \cdots, \frac{\partial U_c}{\partial U_N}\right] \tag{14}$$

The artificial force acts in the direction opposite to the potential gradient; in other words, the force works to decrease the potential. Hence, it has the effect of widening the total altitude gap.

C. OBSTACLE AVOIDANCE CONTROL STRATEGIES

The obstacles encountered during formation flight can be classified into two categories: static and dynamic obstacles. The control scheme for each of these two cases is discussed in the following.

1) THE OBSTACLE IS STATIC

The three UAVs composing the formation system have the same forward velocity in the horizontal plane, and the relative attitude gap between them is close to zero. In addition, the leader and the follower closer to the obstacle form one edge of the triangular formation. This edge is parallel to the obstacle envelope and also to the desired path of the leader. Because the configuration of the formation is fixed, the relative distance between these two curves must be greater than zero to safely avoid the obstacle. The avoidance diagram of the UAVs for the case of a static obstacle is shown in Fig. 4.

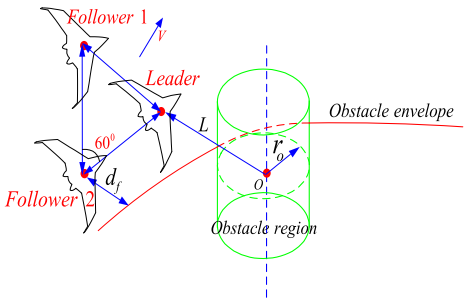

FIGURE 4. The avoidance diagram of the UAV formation for a static obstacle.

Theorem 1: A static obstacle can be successfully avoided when the following condition is satisfied:

$$L - r_0 \geq \xi, \quad d_f - r_0 \geq 0 \tag{15}$$

where ξ is a small positive real parameter, r_0 is the radius of the obstacle region, L is the distance between the leader and the center of the obstacle, and d_f is the distance between the follower and the obstacle envelope.

2) THE OBSTACLE IS DYNAMIC

Suppose that the UAV formation is performing an air strike task, in which the enemy ahead acts as an obstacle, and the UAVs must strike precisely while avoiding this obstacle. The multi-UAV formation has the same forward velocity in three-dimensional space as that of the desired flight trajectory specified by ground command. To prevent the UAV formation from colliding with the target of its movement, the lateral distance between the obstacle and the follower closer to the obstacle must be greater than zero, and the desired trajectory of the UAV formation system must remain dynamically parallel to the envelope of the obstacle to ensure that the UAV formation system will avoid the obstacle and complete its mission successfully. The avoidance diagram for a dynamic obstacle is as shown in Fig. 5.

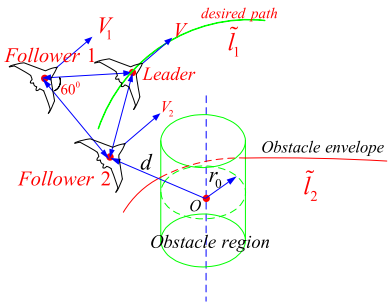

FIGURE 5. The avoidance diagram of the UAV formation for a dynamic obstacle.

Theorem 2: A dynamic obstacle can be successfully avoided when the following condition is satisfied:

$$d - r_0 \geq \zeta, \quad \tilde{l}_1 // \tilde{l}_2 \tag{16}$$

where ξ is a small positive real parameter, r_0 is the radius of the obstacle region, and $\tilde{l}_1$ and $\tilde{l}_2$ denote the desired trajectory of the UAV formation and the envelope of the obstacle, respectively.

In this paper, for a multi-UAV formation system, two collision avoidance control schemes for the two cases described above are proposed based on a leader-follower strategy. In the scheme for a static obstacle, the obstacle avoidance method is relatively simple. The proposed algorithm controls the leader, while a safe distance is maintained between the nearer follower and the obstacle, and the follower tracks the leader to maintain a triangular formation during flight in accordance with the sent formation commands, thereby effectively avoiding a collision. In the other scheme, for a dynamic obstacle, the obstacle avoidance method is more difficult to realize because both the UAV formation system and the obstacle are dynamic. This paper reports numerical simulations of a UAV formation system that were performed to validate the proposed control algorithm. The obstacle avoidance scheme ensures only that the lateral distance between the nearer follower's flight trajectory and the obstacle envelope is no less than some small positive parameter and that the desired trajectory of the UAV formation system remains parallel to the obstacle envelope to ensure flight safety; this approach lays the theoretical foundation for the proposed algorithm.

V. COLLISION AVOIDANCE ALGORITHM

In this section, we further study how to achieve obstacle avoidance for a UAV formation system based on the artificial potential field method and the two collision avoidance schemes presented above to validate the proposed control algorithm, which can achieve collision avoidance both between the UAVs and between the UAVs and obstacles.

A. OBSTACLE AVOIDANCE FOR THE UAV FORMATION SYSTEM

In a triangular UAV formation, each UAV has the same forward velocity and attitude, and the UAVs are located in a plane. Hence, the formation system can be reduced to a rigid body, and a cylindrical obstacle can be reduced to a circle; then, the obstacle avoidance problem can be simplified to that of a particle traveling around a circle on a trajectory that is not tangent to the circle. Whether the obstacle is static or dynamic, the relationship between the particle and the circle must be tangent or non-overlapping to avoid collision between the obstacle and the UAVs. A schematic diagram of the obstacle avoidance problem for the UAV formation system is shown in Fig. 6.

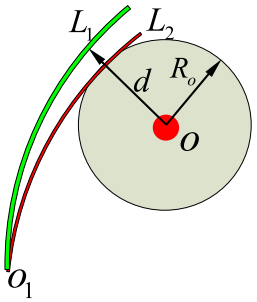

FIGURE 6. Schematic diagram of the obstacle avoidance problem for a UAV formation system.

In Fig.6, o_1 denotes the UAV formation system; o denotes the geometric center of the obstacle; R_o is the radius of the obstacle; L_1 and L_2 are the two trajectories of the UAV formation system at times t_1 and t_2, respectively; and d is the relative distance between L_1 and o. The spatial relationship between the UAV formation system and the obstacle can be expressed as:

$$|d - R_o| \geq 0 \tag{17}$$

Collision avoidance between the UAV formation system and the obstacle is realized only when the inequality in Eq. (20) is satisfied. Because the obstacle avoidance problem for the UAV formation system is basically similar to that discussed in the previous section, we abstain from further description here.

B. COLLISION AVOIDANCE BETWEEN UAVS

For collision avoidance among the UAV formation in three-dimensional space, a control algorithm is proposed to effectively avoid collisions in the vertical direction and in the horizontal plane [10]. In this paper, a consensus-based control algorithm is applied to avoid collisions in the vertical direction only by taking evasive action. However, the triangular formation can fly as directed by the control commands while effectively avoiding collisions between the UAVs. This section mainly studies how to avoid collisions with moving obstacles using the consensus-based algorithm in the vertical direction. For vertical control during the UAV formation flight, the control objectives are roughly grouped into two categories. For the first category, the system comprising the three UAVs together is treated as the control object; for the other, each of the UAVs individually is treated as a control object. The control objective of cooperative formation flight is realized by means of the consensus-based algorithm while maintaining the geometric configuration of the formation. Meanwhile, each of the UAVs can achieve formation flight using the ''leader-follower'' control strategy. The leader provides its own attitude and velocity to its two followers, to which it is directly connected, to ensure that the followers can track the leader while maintaining the triangular formation. The control algorithm proposed in this paper has the advantage of a bidirectional connection topology between the UAVs, and the information transmission between them is smooth, which prevents the exchange of information from clogging due to overload. The control law for UAV i is given by

$$\tilde{T}_{total_i}(t) = -\sum_{j=1}^{N+1} a_{ij}\left[\sum_{k=0}^{1}\gamma_k\left(\hat{h}_i^{(k)} - \hat{h}_j^{(k)}\right)\right], \quad i \in \{1, 2, \cdots, N+1\} \tag{18}$$

$$\hat{h}_j^{(k)} = h_j^{(k)} - h_{h_j}^{(k)}, \quad j \in \{1, 2, \cdots, N+1\},\ k \in \{0, 1\} \tag{19}$$

where N+1 denotes the leader; the $\gamma_k \in R$, $k \in \{0, 1\}$, are control gains; the $h_j^{(k)} \in R$, $k \in \{0, 1\}$, are the states of UAV j; and the $h_{h_j}^{(k)} \in R$, $k \in \{0, 1\}$, are the desired relative states between UAV j and the leader in the vertical direction. As shown in Eq. (6), a_{ij} indicates whether there is information transfer between UAV i and UAV j, when there is information transfer between the UAVs, a_{ij} is set to one, whereas otherwise, a_{ij} is set to zero.

The control algorithm that is proposed in this paper for a UAV formation system with a collision avoidance capability is as follows:

$$\tilde{T}_i = f_{from_i} + f_{ca_i}, \quad i \in \{1, 2, \cdots, N\} \tag{20}$$

where f_{from_i} is the algorithm for controlling the formation in the vertical direction and f_{ca_i} is the obstacle avoidance algorithm based on the artificial potential fields.

Theorem 3: Consider a linear model of a UAV formation system comprising a leader and N (≥ 2) UAVs, as expressed in Eq. (6), and suppose that assumptions (1)-(3) are satisfied. In addition, suppose that Eq. (21) with positive control gains γ_k, $k \in \{0, 1\}$, and Eq. (11) with a positive control parameter k_h are also satisfied for each of the UAVs. Then, all of the states of the UAVs in the vertical direction will asymptotically converge to the desired flight states.

Proof: By applying the control algorithm defined in Eq. (20), we can obtain

$$\dot{h}_i^{(1)} = -\sum_{j=1}^{N+1} a_{ij}\left[\sum_{k=0}^{1}\gamma_k\left(\hat{h}_i^{(k)} - \hat{h}_j^{(k)}\right)\right] + f_{ca_i}, \quad i \in \{1, 2, \cdots, N\} \tag{21}$$

where we define the new force $\bar{f}_{ca} = \left[f_{ca}^T 0\right]^T \in R^{(N+1)}$ and the state vectors $\bar{h}^{(k)} = \left[h_1^{(k)} h_2^{(k)} \cdots h_N^{(k)} 0\right]^T \in R^{(N+1)}$, $k \in \{0, 1\}$, $\hat{h}^{(k)} = \left[\hat{h}_1^{(k)} \hat{h}_2^{(k)} \cdots \hat{h}_{N+1}^{(k)}\right]^T \in R^{(N+1)}$. Using this newly defined notation, we can rewrite Eq. (21) as follows:

$$\dot{\hat{h}}^{(1)} = -\gamma_o L\hat{h}^{(0)} - \gamma_1 L\hat{h}^{(1)} + \bar{f}_{ca} \tag{22}$$

where the matrix L is the graph Laplacian of the multi-UAV system and the state vector $\hat{h}^{(k)}$ consists of the states of the followers and the commands from the leader. In this paper, the following identities concerning the rows of the graph Laplacian L hold:

$$\begin{cases} a_i\,(N+1) = \sum_{j=1}^{N+1} a_{ij} - a_{i1} - a_{i2} - \cdots - a_{iN} \\ a_{ii} = 0, \quad i \in \{1, 2, \cdots, N\} \end{cases} \tag{23}$$

Using $d_{N+1}^{(k)} = 0$, $k \in \{0, 1\}$, and Eq. (23), Eq. (22) can be expressed as

$$\begin{aligned} \dot{h}^{(1)} = &-\gamma_0 M h^{(0)} - \gamma_0 M h^{(0)} + \gamma_0 M \tilde{h}_{N+1}^{(0)} + \gamma_1 M \tilde{h}_{N+1}^{(0)} \\ &+ \gamma_0 M d_h^{(0)} + \gamma_0 M d_h^{(0)} + f_{ca} \end{aligned} \tag{24}$$

where the matrix $M \in R^{N\times N}$ is defined as shown in Eq. (25) and the state vectors $h^{(k)}$ and $\tilde{h}_{N+1}^{(k)}$ are $h^{(k)} = \left[h_1^{(k)} h_2^{(k)} \cdots h_N^{(k)}\right]^T$ and $\tilde{h}_{N+1}^{(k)} = 1_N \otimes h_{N+1}^{(k)} \in R^N$, respectively. Here, $\otimes$ denotes the Kronecker product, and $1_N = [11\cdots1]^T \in R^N$. The matrix M is similar but not equal to the graph Laplacian.

$$M = \begin{bmatrix} \sum_{j=1}^{N+1} a_{1j} & -a_{12} & \cdots & a_{1N} \\ a_{21} & \sum_{j=1}^{N+1} a_{2j} & \cdots & a_{2N} \\ \vdots & \vdots & \ddots & \vdots \\ a_{Nj} & a_{Nj} & \cdots & \sum_{j=1}^{N+1} a_{Nj} \end{bmatrix} \tag{25}$$

Using the matrix M and Eq. (18), Eq. (6) can be simplified to matrix-vector form as follows:

$$\begin{aligned} \frac{d}{dt}\begin{bmatrix} h^{(0)} \\ h^{(1)} \end{bmatrix} = &\begin{bmatrix} 0_N & I_N \\ -\gamma_0 M & -\gamma_1 M \end{bmatrix}\begin{bmatrix} h^{(0)} \\ h^{(1)} \end{bmatrix} + \begin{bmatrix} 0_N \\ f_{ca} \end{bmatrix} \\ &+ \begin{bmatrix} 0_N & I_N \\ \gamma_0 M & \gamma_1 M \end{bmatrix}\begin{bmatrix} \tilde{h}_{N+1}^{(0)} \\ \tilde{h}_{N+1}^{(1)} \end{bmatrix} \\ &+ \begin{bmatrix} 0_N & I_N \\ \gamma_0 M & \gamma_1 M \end{bmatrix}\begin{bmatrix} d_h^{(0)} \\ d_h^{(1)} \end{bmatrix} \end{aligned} \tag{26}$$

where $I_N \in R^{N\times N}$ is an N-dimensional unit matrix and $0_N \in R^N$ is an N-dimensional zero vector.

To validate the stability of Eq. (26), this equation can be expressed in homogeneous form as

$$\frac{d}{dt}\begin{bmatrix} h^{(0)} \\ h^{(1)} \end{bmatrix} = \begin{bmatrix} 0_N & I_N \\ -\gamma_0 M & -\gamma_1 M \end{bmatrix}\begin{bmatrix} h^{(0)} \\ h^{(1)} \end{bmatrix} + \begin{bmatrix} 0_N \\ f_{ca} \end{bmatrix} \tag{27}$$

Here, we construct a Lyapunov candidate function V that represents the total energy of the multi-UAV system. The expression is shown below:

$$V = \frac{1}{2}\dot{h}^T\dot{h} + \frac{1}{2}\gamma_0 h^T M h + U_c \tag{28}$$

The time derivative of the function V is given by

$$\dot{V} = \dot{h}^T\left(\ddot{h} + \gamma_0 M h\right) + \dot{U}_c = -\gamma_1 \dot{h}^T M \dot{h} + \dot{h}^T f_{ca} + \dot{U}_c \tag{29}$$

From Eq. (11), we can obtain Eq. (30):

$$\dot{U}_c = \dot{h}^T \nabla U_c = -\gamma_1 \dot{h}^T f_{ca} \tag{30}$$

Then, from Eq. (29) and Eq. (30), we can obtain

$$\dot{V} = -\gamma_1 \dot{h}^T M \dot{h} \tag{31}$$

The Lyapunov candidate function V represents the energy of the artificial field acting among the UAVs in the system. Through studying the function V, we can endow the UAV formation system with a collision avoidance capability to achieve effective control from the ground station for the purpose of avoiding obstacles. The graph G has a directed spanning tree if assumptions (1)-(3) hold. Hence, according to the properties of the graph Laplacian, L has a single eigenvalue of zero, and the other eigenvalues have a positive real part. According to the properties of and the relationship between L and M, we can find that the matrix M is positive definite. In addition, the artificial potential field parameter K_h has a positive value, meaning that $U_c \geq 0$. Therefore, when the control gain γ_0 and k_h are positive simultaneously, we obtain $V \geq 0$, and when the control gain γ_0 and k_h are zero simultaneously, we obtain $V = 0$. Moreover, when $h = 0$, $\dot{h} = 0$, and $U_c = 0$, we again obtain $V = 0$. Note that we obtain $U_c = 0$ when there is no overlap between the safe regions of the UAVs.

Regarding the derivative of the Lyapunov candidate function $\dot{V}$, we obtain $\dot{V} \leq 0$ when the control gain γ_1 is positive and $M > 0$. We obtain $\dot{V} = 0$ if $h = 0$, $\dot{h} = 0$, and $U_c = 0$; otherwise, $\dot{V} \neq 0$. We can solve for the asymptotic stability condition by using the Lyapunov theorem and invoking LaSalle's principle [26].

When there is no overlap of the safe regions, the particular solution to Eq. (26) is given by

$$\begin{bmatrix} h^{(0)} \\ h^{(1)} \end{bmatrix} = \begin{bmatrix} \tilde{h}_{N+1}^{(0)} \\ \tilde{h}_{N+1}^{(1)} \end{bmatrix} + \begin{bmatrix} d_h^{(0)} \\ d_h^{(1)} \end{bmatrix} \tag{32}$$

The validity of this solution can be confirmed by substituting Eq. (32) into Eq. (26), so there is no need to further explain it. Because the leader provides the desired commands to each follower, instead of the desired input commands, we can use $\tilde{h}_{N+1}^{(2)} = 0$ and $d_h^{(2)} = 0$. Note that $\tilde{h}_{N+1}^{(2)} = 0$ and $d_h^{(2)} = 0$ are the input to the leader and the input error between the leader and the follower, respectively.

In conclusion, the general solution to the non-homogeneous differential equation given as Eq. (26) is the sum of the general solution to the homogeneous equation and

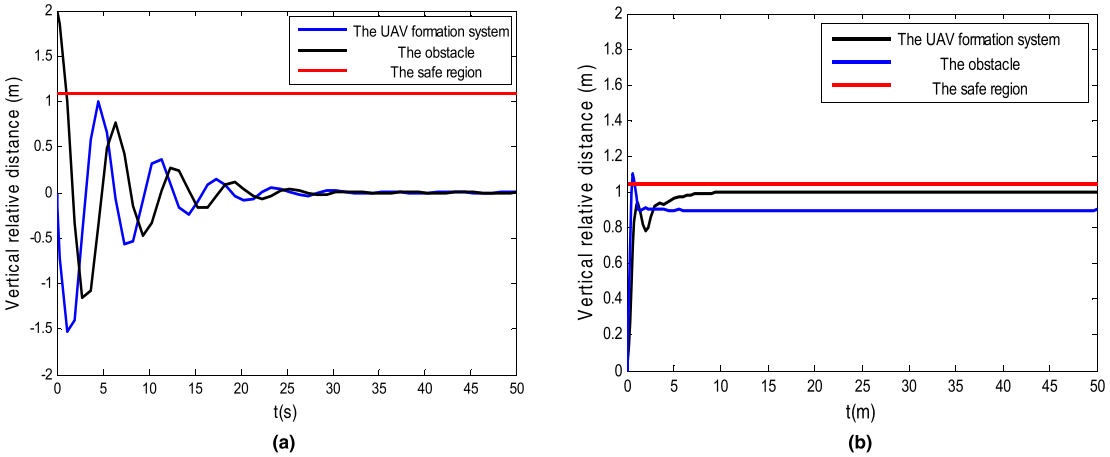

FIGURE 7. The vertical relative distance of the UAV formation system. (a) Without the collision avoidance algorithm. (b) With the collision avoidance algorithm.

the particular solution. Hence, the general solution to Eq. (26) asymptotically converges to Eq. (33) when the control gains γ_k, $k \in \{0, 1\}$, and the artificial potential field parameter k_h are chosen to have small positive values.

$$\begin{bmatrix} h^{(0)} \\ h^{(1)} \end{bmatrix} \to \begin{bmatrix} \tilde{h}^{(0)}_{N+1} \\ \tilde{h}^{(1)}_{N+1} \end{bmatrix} + \begin{bmatrix} d^{(0)}_h \\ d^{(1)}_h \end{bmatrix}, \quad \text{as } t \to \infty \qquad (33)$$

From the Eq. (33), we can obtain the result regarding the convergence to the commands issued by the leader. According to the element of the first row block in Eq. (23), it is proven that every UAV has the capability of collision avoidance and can asymptotically converge to the desired trajectory for triangular formation flight.

VI. SIMULATION RESULTS AND ANALYSIS

In this section, we present the simulation tests performed to validate the proposed consensus-based control algorithm.

A. THE INITIAL CONDITIONS

We considered a triangular UAV formation composed of three UAVs, including a leader and two followers. A moving obstacle was simplified to a cylindrical region, as shown in Fig. 5. In addition, the UAV formation model was simplified to a simple network topology with a directed spanning tree, and it was assumed that each of the UAVs could communicate with each other (i.e., bidirectional transmission between the UAVs was assumed). The leader was assumed to maintain a constant altitude of 600 m and a relative altitude of 1.2 m between the leader and the followers, with a relative altitude error of zero. At the same time, the leader provided a desired relative altitude of $d_{h_i} = 0, \forall i \in \{1, 2\}$.

To effectively validate the proposed control algorithm via simulation experiments, we adopted the following assumptions:

1) The forward velocity and direction of the UAV in the model depicted in Fig. 5 are constant.

2) The posture and position of the leader are controlled from the ground station.

3) The communication between the leader and the follower is synchronous.

The relative ground velocity of the UAVs and the velocity of the obstacle are both 56 m/s, the mass of each of the UAVs is 90 kg, the pitch rate limit for the UAVs is 10 deg/s, and the yaw rate limit for the UAVs is 12 deg/s. To satisfy the formulated model and simulate all conditions in the vertical direction, we established control gains of $\gamma_0 = 1.5$ and $\gamma_1 = 3$ and a collision control parameter of $k_h = 5.5$. The height of the safe region for every UAV was set to 3 m, the radius of each safe region was set to 3.5 m, the altitude gap between them was constrained to be no more than 1.2 m, and the relative distance between them was constrained to be no more than 10 m. To validate the proposed control algorithm, two sets of simulation experiments were conducted, with and without the collision avoidance algorithm.

B. SIMULATION RESULTS AND ANALYSIS

In Figs. 7 to 10, we present the simulation results with the initial conditions and assumptions described above. Figs. 7 to 9 present the collision avoidance diagrams of the UAV formation system. Fig. 10 presents the collision avoidance trajectory diagrams of UAVs controlled with the different algorithms. Meanwhile, panels (a) and (b) of Figs. 7 to 8 present the simulation results without and with the collision avoidance algorithm, respectively.

As seen from Fig. 7(a), the curves corresponding to the obstacle and the UAV formation system show a trend of oscillating attenuation that eventually converges to zero. A collision can easily occur between them if the relative vertical distance is zero, and there is an overlap between the safe region of the UAV formation system and the obstacle region in the horizontal plane. However, with the control algorithm, a collision can be effectively avoided. From Eq. (24), we find that the vertical distance converges to a small positive value

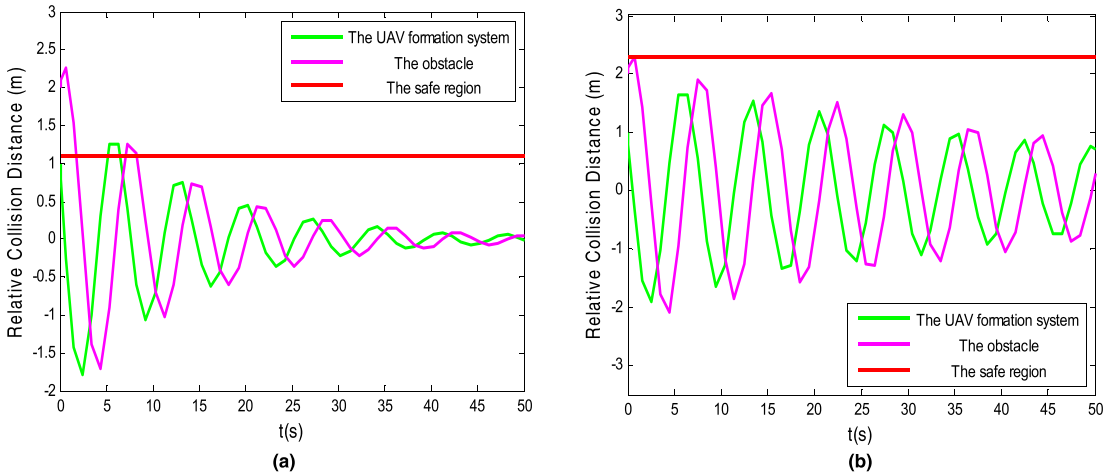

FIGURE 8. The relative collision avoidance distance between the UAV formation system and the obstacle. (a) Without the collision avoidance algorithm. (b) With the collision avoidance algorithm.

for a sufficiently long simulation time; i.e., the distance between the UAV formation and the obstacle remains at a constant positive value in Fig. 7(b), as desired, successfully avoiding a collision.

Fig. 8(a) shows that the relative collision avoidance distance is less than the desired value, and the curve presents an oscillatory convergence trend until the relative distance between the obstacle and the formation converges to zero. However, a collision is most likely to occur under these conditions. Fig. 8(b) shows the UAVs still maintain their triangular formation in flight, whereas the obstacle flies at a constant forward velocity and in a constant direction. Hence, the UAV formation system can effectively avoid collision by means of the collision avoidance control algorithm.

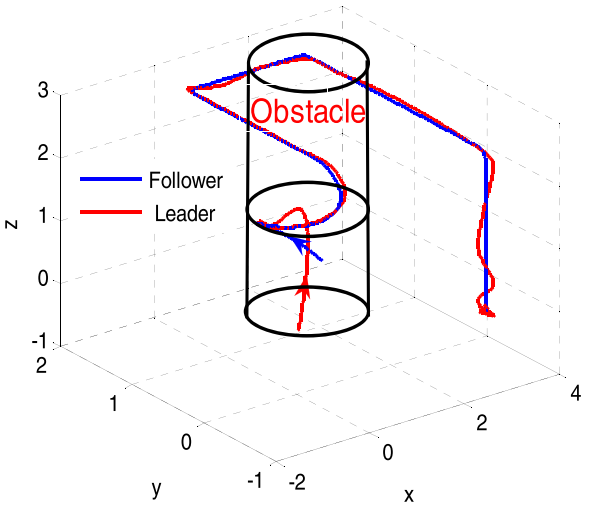

FIGURE 9. The collision avoidance diagram of the "leader-follower" control strategy.

Fig. 9 shows the collision avoidance process of a two-UAV formation maneuvering via the "leader-follower" control strategy in three-dimensional space. As seen from

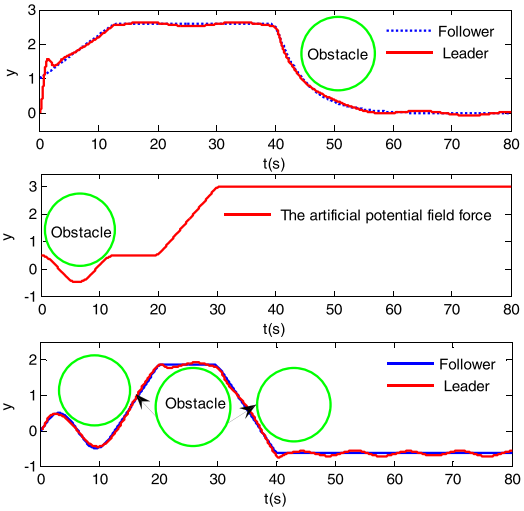

FIGURE 10. The collision avoidance trajectory diagrams of UAVs controlled with the different algorithms.

Fig. 10, based on the artificial potential field method with a three-dimensional spatial rotation vector, the UAV formation system can avoid the obstacle with a smooth trajectory close to the obstacle and then assemble into the desired triangular formation to track the motion of the target until the target point is reached under the "leader-follower" control strategy. During collision avoidance, the UAV formation system can maintain good stability and robustness, thus verifying the effectiveness and feasibility of the proposed control algorithm.

Fig. 10 compares the UAV collision avoidance trajectories generated using the general collision avoidance control algorithm, the improved artificial potential field method and the three-dimensional composite artificial potential field method. With a three-dimensional composite artificial potential field, the UAV can avoid the obstacle along the optimal path while maintaining good stability and robustness throughout the entire process of continuous collision avoidance.

Based on the above analysis, the proposed control strategies can effectively avoid collisions between the UAVs and between the UAV formation system and an obstacle, as seen from a comparative analysis of simulation experiments, and can theoretically achieve the intended purpose of collision avoidance. The proposed collision avoidance scheme is based on two principles. The first is that a collision avoidance algorithm combined with an artificial potential field is applied to avoid collisions in the vertical direction; the second is that an artificial potential field alone is applied to avoid collisions in the horizontal plane.

VII. CONCLUSION

The consensus-based algorithm and a ''leader-follower'' control strategy are simultaneously designed for application to the complicated collision avoidance problem in three-dimensional space, which can be simplified to dual problems of collision avoidance control in the horizontal plane and in the vertical direction. When the relative distance between any two UAVs in the formation is less than the safe distance in the vertical direction, evasive maneuvers must be taken to avoid a collision. In addition, the artificial potential field method is applied to avoid collisions within the UAV formation in the horizontal plane. When the relative distance between any two UAVs in the formation is less than the safety margin, a repulsive force will be produced; otherwise, an attractive force is produced. Eventually, the UAV formation system reaches an equilibrium state and forms a triangular formation in flight.

REFERENCES

[1] Y. He, F. R. Yu, N. Zhao, H. Yin, H. Yao, and R. C. Qiu, ''Big data analytics in mobile cellular networks,'' *IEEE Access*, vol. 4, pp. 1985–1996, 2016.

[2] G. M. Atinç, D. M. Stipanović, P. G. Voulgaris, and M. Karkoub, ''Collision-free trajectory tracking while preserving connectivity in unicycle multi-agent systems,'' in *Proc. Amer. Control Conf.*, Jun. 2013, pp. 5392–5397.

[3] T. Wang, H. Gao, and J. Qiu, ''A combined adaptive neural network and nonlinear model predictive control for multirate networked industrial process control,'' *IEEE Trans. Neural Netw. Learn. Syst.*, vol. 27, no. 2, pp. 416–425, Feb. 2016.

[4] Z. Wang, G. Wu, and M. J. Barth, ''Developing a distributed consensus-based cooperative adaptive cruise control system for heterogeneous vehicles with predecessor following topology,'' *J. Adv. Transp.*, vol. 2017, Aug. 2017, Art. no. 1023654.

[5] J. Biswas, M. A. Kamath, K. G. Anjana, and M. Barai, ''Design, architecture and real time distributed coordination DMPPT algorithm for PV systems,'' *IEEE J. Emerg. Sel. Topics Power Electron.*, to be published.

[6] W. Ren, ''Consensus tracking under directed interaction topologies: Algorithms and experiments,'' *IEEE Trans. Control Syst. Technol.*, vol. 18, no. 1, pp. 230–237, Jan. 2010.

[7] Z. Meng, W. Ren, Y. Cao, and Z. You, ''Leaderless and leader-following consensus with communication and input delays under a directed network topology,'' *IEEE Trans. Syst., Man, Cybern. B, Cybern.*, vol. 41, no. 1, pp. 75–88, Feb. 2011.

[8] C. Yoshioka and T. Namerikawa, ''Observer-based consensus control strategy for multi-agent system with communication time delay,'' in *Proc. IEEE Int. Conf. Control Appl.*, Sep. 2008, pp. 1037–1042.

[9] H. Kawakami and T. Namerikawa, ''Cooperative target-capturing strategy for multi-vehicle systems with dynamic network topology,'' in *Proc. Amer. Control Conf.*, Jun. 2009, pp. 635–640.

[10] Y. Kuriki and T. Namerikawa, ''Formation control of UAVs with a fourth-order flight dynamics,'' in *Proc. 52nd IEEE Conf. Decis. Control*, Dec. 2014, pp. 6706–6711.

[11] Y. Kuriki and T. Namerikawa, ''Consensus-based cooperative formation control with collision avoidance for a multi-UAV system,'' in *Proc. Amer. Control Conf.*, Jun. 2014, pp. 2077–2082.

[12] G. Jennifer, R. Rahul, and S. Kamesh, ''Aircraft conflict detection and resolution using mixed geometric and collision cone approaches,'' *AIAA J.*, 2004.

[13] H. Choi, Y. Kim, and I. Hwang, ''Vision-based reactive collision avoidance algorithm for unmanned aerial vehicle,'' in *Proc. AIAA Guid., Navigat., Control Conf.*, 2013.

[14] E. Portilla *et al.*, ''Sense and avoid (SAA) & traffic alert and collision avoidance system (TCAS) integration for unmanned aerial systems (UAS),'' in *Proc. AIAA Infotech Aerosp. Conf. Exhib.*, 2006.

[15] G. Fasano, D. Accardo, and A. Moccia, ''Multi-sensor-based fully autonomous non-cooperative collision avoidance system for unmanned air vehicles,'' *J. Aerosp. Comput., Inf., Commun.*, vol. 5, no. 10, pp. 338–360, 2008.

[16] Y. Kuriki and T. Namerikawa, ''Control of formation configuration using leader-follower structure,'' *J. Syst. Des. Dyn.*, vol. 7, no. 3, pp. 254–264, 2013.

[17] T. H. Summers, M. R. Akella, and M. J. Mears, ''Coordinated standoff tracking of moving targets: Control laws and information architectures,'' *J. Guid. Control Dyn.*, vol. 32, no. 1, pp. 56–69, 2013.

[18] T. S. Andersen and R. Kristiansen, ''Path-following in three dimensions using quaternions for a fixed-wing UAV,'' in *Proc. IEEE 26th Int. Symp. Ind. Electron. (ISIE)*, Jun. 2017, pp. 1117–1122.

[19] B. Fang, X. F. Feng, and X. Shuo, ''Research on cooperative collision avoidance problem of multiple UAV based on reinforcement learning,'' in *Proc. 10th Int. Conf. Intell. Comput. Technol. Automat. (ICICTA)*, Oct. 2017, pp. 103–109.

[20] Y. Lin and S. Saripalli, ''Sampling-based path planning for UAV collision avoidance,'' *IEEE Trans. Intell. Transp. Syst.*, vol. 18, no. 11, pp. 3179–3192, Nov. 2017.

[21] Y. Kuriki and T. Namerikawa, ''Experimental validation of cooperative formation control with collision avoidance for a multi-UAV system,'' in *Proc. 6th Int. Conf. Automat., Robot. Appl.*, Feb. 2015, pp. 531–536.

[22] J. Zhang *et al.*, ''The collision avoidance control algorithm of the UAV formation flight,'' in *Proc. ARAA*, 2017, pp. 1–7.

[23] C. Li and Z. H. Qu, ''Distributed finite-time consensus of nonlinear systems under switching topologies,'' *Automatica*, vol. 50, no. 6, pp. 1626–1631, 2014.

[24] Z. H. Qu, C. Y. Li, and F. Lewis, ''Cooperative control with distributed gain adaptation and connectivity estimation for directed networks,'' *Int. J. Robust Nonlinear Control*, vol. 24, no. 3, pp. 450–476, 2014.

[25] J. Peng, C. Li, and X. Ye, ''Cooperative control of high-order nonlinear systems with unknown control directions,'' *Syst. Control Lett.*, vol. 113, pp. 101–108, Mar. 2018.

[26] H. K. Khalil, *Nonlinear Systems*. Upper Saddle River, NJ, USA: Prentice-Hall, 2001.

JIALONG ZHANG received the B.Eng. degree from the North China Institute of Aerospace Engineering in 2014 and the M.E. degree from the College of Aeronautics and Astronautics Engineering, Air Force Engineering University, in 2017. He is currently pursuing the Ph.D. degree with the School of Automation, Northwestern Polytechnical University. His main research interest lies in cooperative UAV formation flight control.

JIANGUO YAN received the B.Eng. degree from the College of Astronautics Engineering, National University of Defense Technology, in 1983, and the Ph.D. degree from the School of Automation Control, Northwestern Polytechnical University, in 2007. His research interests include computer control and intelligent control, pattern recognition, robust control, navigation, guidance and flight control, and optical flight control.

PU ZHANG received the B.Eng. and M.Eng. degrees from the North China Institute of Aerospace Engineering in 2008 and 2012, respectively. She is currently pursuing the Ph.D. degree with Northwestern Polytechnical University. Her main research interests lie in management and optimization.

XIANGJIE KONG received the B.Eng. degree from the College of Information Science and Engineering, Zhejiang University, Hangzhou, China, in 2004, and the Ph.D. degree from the School of Software, Dalian University of Technology, Dalian, China, in 2009, respectively. He is currently an Associate Professor with the School of Software, Dalian University of Technology. His interests lie in big date, mobile computing, and computational social science.